Environmental Science & Technology Letters

pubs.acs.org/journal/estlcu

Letter

Cysteine-Protected Antibacterial Spheroids of Atomically Precise Copper Clusters for Direct and Affordable Arsenic Detection from Drinking Water

Jenifer Shantha Kumar, Arijit Jana, Jayathraa Raman, Hema Madhuri Veera, Amoghavarsha Ramachandra Kini, Jayoti Roy, Saurav Kanti Jana, Tiju Thomas, and Thalappil Pradeep*

Cite This: https://doi.org/10.1021/acs.estlett.4c00264

Read Online

ACCESS | Metrics & More | Article Recommendations | Supporting Information

ABSTRACT: Rapid and naked-eye detection of water-borne contaminants using molecularly precise nanomaterials has emerged as a promising strategy to reduce the impact of chemical pollution. This study presents a luminescence-based arsenic (*As*) sensor, eliminating the need for sample preparation. Incorporating red-emitting spheroidal cluster-assembled superstructures (CASs), comprised of Cu_{17} nanoclusters (Cu_{17}NCs), coprotected by L-cysteine (L-Cys) and 1,2-bis(diphenylphosphino) ethane (DPPE) ligands, the sensor exhibits notable sensitivity toward arsenite (As^{3+}) and (As^{5+}) ions. A detection limit of 1 ppb in tap water was achieved through luminescence-based quenching. Remarkably, it demonstrates selective detection of *As* amidst common interfering metal ions such as Cd^{2+}, Hg^{2+}, Fe^{3+}, Pb^{2+}, Cu^{2+}, and Cr^{3+}. A sensor disc made of CASs coated on nonwoven polypropylene (PP) mats has been devised for practical field applications. Electron microscopy reveals disrupted morphology of the spheroids due to *As* interaction. Moreover, the CASs exhibit significant antibacterial efficacy against Gram-negative *Escherichia coli* and Gram-positive *Staphylococcus aureus* and antibiofilm properties against *Bacillus subtilis*. This research highlights the effectiveness of atomically precise clusters for a practical application with direct societal relevance.

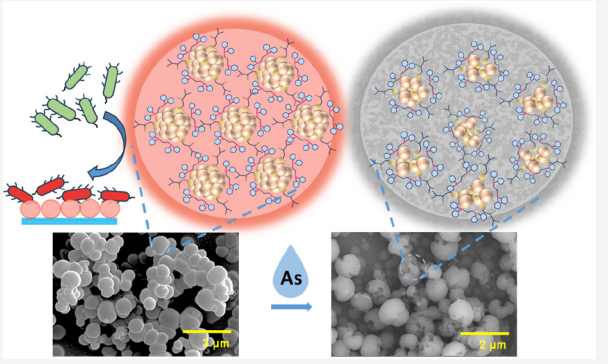

KEYWORDS: *Nanocluster assembly, Cu_{17} nanoclusters, Red luminescence, Arsenic, Sensing, Antibacterial, Antibiofilm*

1. INTRODUCTION

One-third of the human population is deprived of access to safe drinking water.[1] Contaminants in water include metal ions and microorganisms, such as bacteria, fungi, protozoa and viruses. Arsenic (*As*) is one of the most hazardous heavy metals (although semimetal technically) prevalent in diverse water sources, which is identified as the largest mass poisoning in the history of humanity.[2,3] Most regulating agencies have fixed the *As* limit at 10 ppb in drinking water.[4,5] Quantifying *As* at ppb levels using portable, solid-state sensors has also been challenging.[6] Lack of an efficient sensing system which is selective, affordable, and easy to handle, particularly in the field, persists.[7] Also, it is crucial to develop sensing systems capable of detecting both ionic states, considering that inorganic *As* exists as arsenite (As^{3+}) and arsenate (As^{5+}) ions. As^{3+} is predominant in water at reducing conditions such as groundwater, whereas As^{5+} is present in surface waters.[8] Recently, several promising heavy metal sensing systems based on nanoclusters (NCs) have been developed.[9−11] NCs are a new class of atomically confined materials carrying fewer atoms than nanoparticles and consequently have a higher surface-to-volume ratio with interesting chemical and photophysical properties.[9−13] To date, gold and silver are the preferred NCs due to their facile synthesis, wide range of photophysical properties and stability in ambient conditions.[14] Copper NCs (CuNCs) are nonprecious metal alternatives, more economically viable than NCs of gold, silver, and platinum, exhibiting many versatile applications and are highly biocompatible.[9,14] They are more readily available and have fascinating optical properties.[14] CuNCs-based luminescence sensors have advantages, such as enhanced quantum yield and tunable excited states.[15] Affordability in the field is an important criterion, especially in resource-limited situations. Aggregation-induced emission (AIE) often observed in CuNCs enhances the emission brightness, structural stability, and sensitivity of CuNCs-assembled solids.[16,17] Some reports on metal NCs based sensors for *As* detection are available, explicitly involving

Received: April 5, 2024
Revised: June 23, 2024
Accepted: June 25, 2024

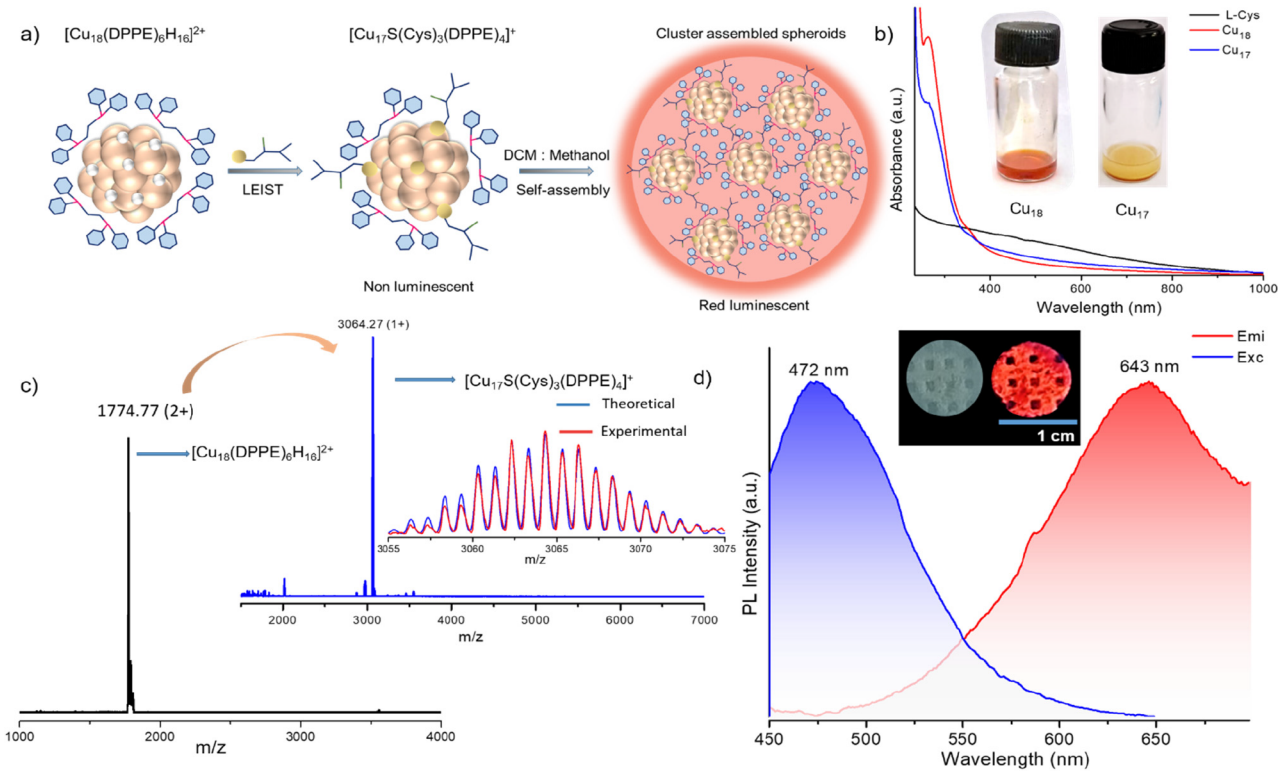

Figure 1. (a) Schematic representation of the synthesis of L-Cys and DPPE-protected Cu_{17}NCs and the self-assembly of the cluster in DCM:methanol (1:1, v/v) solvent mixture. (b) Comparative UV−vis absorption spectra of L-Cys, Cu_{18}, and Cu_{17}NCs. Inset shows the photographs of the respective clusters. (c) Full range ESI MS spectrum of the Cu_{18}NCs and the Cu_{17}NCs in positive ion mode. The inset matches the isotopic distribution of the experimental (blue) and theoretical (red) spectra of Cu_{17}NCs. (d) Photoluminescence excitation and emission spectra of Cu_{17}NCs covered on a PP disc. The inset shows the photograph of the CASs coated on PP mats under daylight (left) and UV light (right).

electrochemical[18,19] and luminescence[20,21] responses. A recent report from our group demonstrated that cobalt NCs-assembled plates detect As^{3+} in water electrochemically, with high sensitivity and selectivity.[19] However, luminescence sensors generally offer higher sensitivity toward the analytes over other techniques.[22] Luminescent gold and silver NCs have been demonstrated to show selective detection of *As* at levels far below the permissible limits.[20,21] To our knowledge, there is no report of CuNCs for *As* sensing.[23] In this study, we present a sensor composed of red-emitting cluster-assembled superstructures (CASs) of Cu_{17}NCs, which can detect both As^{3+} and As^{5+} ions in tap water at the ppb level with high selectivity. CASs showed disrupted morphology upon exposure to *As* and subsequent change in emission, forming the basis of sensing.

Besides heavy metal ions, microbial organisms cause immediate and severe health issues worldwide. The Centres for Disease Control and Prevention has expressed that the world is entering a "postantibiotic era", where mortality will be primarily due to resistant-bacterial diseases.[24,25] With challenges faced in disinfection, NCs are emerging as novel antimicrobials. Silver[26] and CuNCs possess high antibacterial activity.[27] Very few studies on CASs are available.[27,28] The CASs reported here exhibit excellent antibacterial activity against Gram-negative and Gram-positive bacteria in water, showcasing their potential applications as broad-spectrum of antibacterial coatings. They also exhibit biofilm resistance.

2. METHODS AND MATERIALS

Materials and Reagents. Copper iodide (CuI), sodium borohydride ($NaBH_4$, 98%) and L-cysteine (L-Cys) were procured from Sigma-Aldrich chemicals. DPPE was supplied by Rankem Chemicals. Solvent-grade dichloromethane (DCM), acetonitrile and methanol (99.5%) were purchased from Finar, India. Sodium arsenite and sodium arsenate were purchased from Aldrich Chemicals. Nutrient agar (NA) and Luria−Bertani (LB) Broth were purchased from Himedia.

Experimental Procedures. The Cu_{17}NCs were synthesized from Cu_{18}NCs using the (Ligand-exchange- induced structural transformation) LEIST method (Figure 1a).[29] Details of the syntheses of Cu_{18} and Cu_{17}NCs are furnished in Text S1 and S2, respectively. The sensing experiments are discussed in Text S3.

Details of the antibacterial experiments and analytical methods used in this work are presented in Texts S4 and S5, respectively.

3. RESULTS AND DISCUSSION

Arsenic Sensing Ability of Cu_{17}NCs CASs. The synthesis of the Cu_{17}NCs through a ligand exchange reaction starting from Cu_{18}NCs is schematically shown in Figure 1a and characterization of the Cu_{17}NCs is discussed in Text S6 and Figures 1b-d, Figures S1−3. To create the *As*-sensing films, Cu_{17}NCs solution was drop-cast onto nonwoven Polypropylene (PP) discs and left to dry at room temperature. The inset of Figure 1d displays photographs of Cu_{17}NCs coating on PP discs under daylight and UV light. Bright red luminescence was

https://doi.org/10.1021/acs.estlett.4c00264
Environ. Sci. Technol. Lett. XXXX, XXX, XXX−XXX

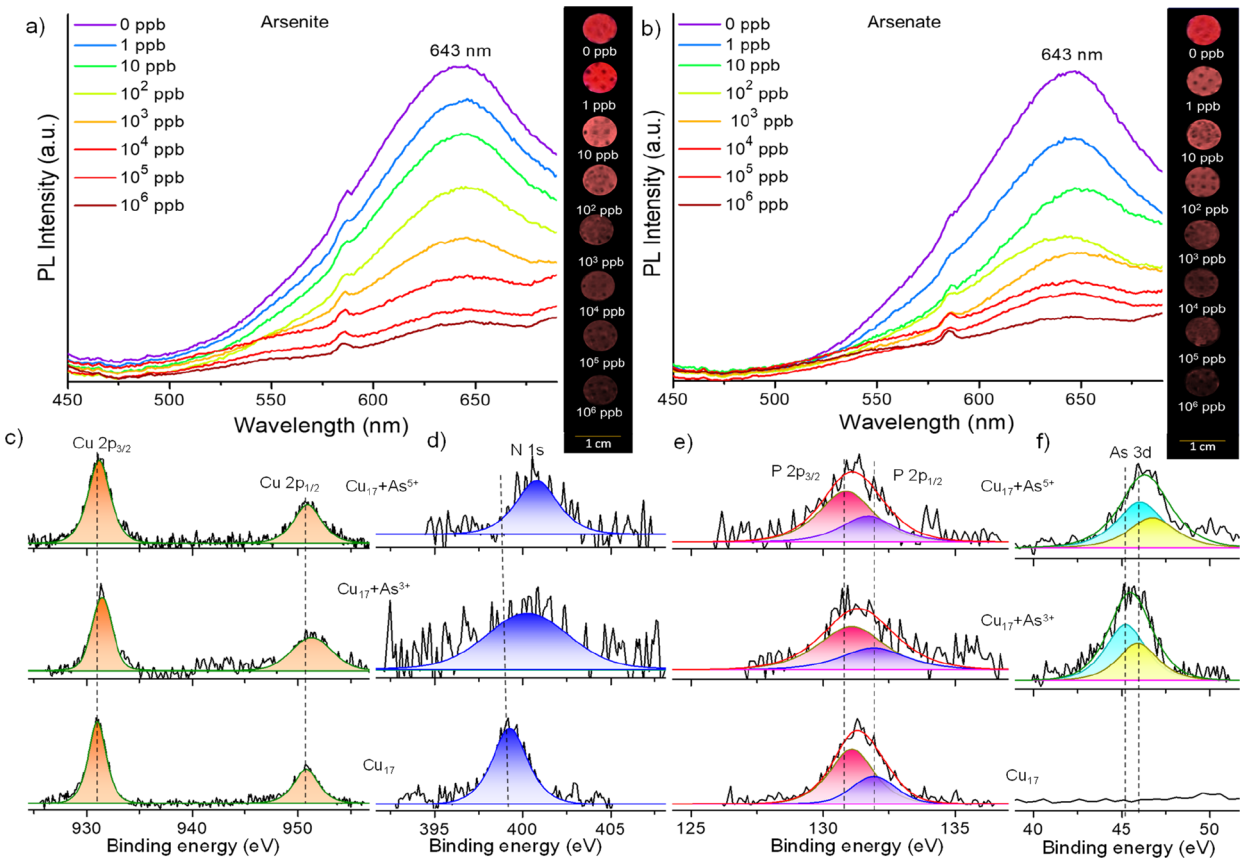

Figure 2. Comparative PL spectra with increasing concentrations of (a) As^{3+} and (b) As^{5+} ions showing the gradual quenching of PL intensity of the PP disc coated with Cu_{17} NCs. Correlative XPS spectra of Cu_{17} NCs having (c) Cu 2p, (d) N 1s, (e) P 2p, and (f) *As* 3d regions.

observed for the coatings under UV light, which was weak in the NCs solution. Upon investigating the Cu_{17}NCs coatings through a photoluminescence (PL) spectrophotometer, an emission maximum at 643 nm was observed with an excitation at 472 nm (Figure 1d). The spectral maximum of Cu_{17}NCs in DCM: Methanol (1:1) solution is blue-shifted (613 nm) compared to the coating (Figure S4). The emission intensity was also observed to be lower in solution. This indicated the AIE enhancement in the coatings compared to the as-prepared NCs.

The Cu_{17}NCs coating exhibited sensitivity to *As*, displaying a quenching of the red luminescence upon exposure to As^{3+} or As^{5+} in water (insets of Figures 2a and 2b). The sensor demonstrated the ability to detect both the analytes down to 1 ppb, starting from 10^6 ppb (Figures 2a and b). The correlation coefficient values are R^2 = 0.98 and 0.99 for As^{3+} and As^{5+}, respectively (Figures S5 a and b). The performance of Cu_{17}NCs in *As* sensing has been compared in Table S1 with the existing reports, and the sensors' affordability is discussed in Text S6.

To further investigate the sensing ability toward *As* X-ray photoelectron spectroscopy (XPS) analysis was performed on the NCs exposed to As^{3+} and As^{5+} ions. Before and after exposure to *As*, the NCs were loaded onto clean XPS stubs. The recorded survey spectrum displayed all the elements in the Cu_{17}NCs (Figure S6a). Detailed scans reveal peaks corresponding to Cu $2p_{3/2}$ and Cu $2p_{1/2}$ at 932.9 and 952.8 eV, respectively, indicating zero oxidation state of Cu in the NCs (Figure 2c).[30] Upon interaction with As^{3+} and As^{5+}, Cu $2p_{3/2}$ peak shifted toward lower binding energy (931.3 and 931.1 eV, respectively), indicating oxidation of Cu. Similar shifts were observed in the Cu $2p_{1/2}$ peak upon exposure to As^{3+} and As^{5+} (from 952.8 to 951.3 and 950.9 eV, respectively), along with substantial broadening, confirming oxidation. Peaks of N 1s, P $2p_{3/2}$ and P $2p_{1/2}$ showed broadening, indicating their involvement in *As* sensing (Figures 2d and 2e). Figure 2f shows the presence of *As* in the cluster after adding As^{3+} and As^{5+}, compared to the Cu_{17}NCs. Sulfur exhibits a similar effect on adding *As*, wherein it undergoes oxidation (Figure S6b). Oxygen 1s region shows slight shifts, confirming the impact of *As* on oxygen present in the protecting ligands in the NCs (Figure S6c). Previous reports on *As*-specific sensing systems highlighted the role of amino groups in binding with *As*.[31,32] XPS data confirmed the interaction of both the ligands, DPPE and L-Cys, to *As*. This comprehensive investigation revealed that exposure to *As* alters the Cu core and ligands of the NCs.

Furthermore, Fourier-transform infrared (FTIR) analysis was conducted to elucidate the binding interaction between *As* and Cu_{17}NCs. The FT-IR spectrum of the NCs revealed a set of vibrational features at 1574 and 1617 cm^{-1} corresponding to the stretching and bending vibrations of C═O and NH_2 groups, respectively, of the L-Cys ligand.[33] These peaks exhibit decreased intensity and broadening following interaction with As^{3+} (Figure S7a) or As^{5+} ions (Figure S7b). The peak at 1724 cm^{-1}, corresponding to the C═O stretching mode, similarly displays a declining intensity trend, confirming the interaction with *As*. Additionally, a decrease in intensity was observed for C−O at 1190 and 1250 cm^{-1} upon exposure to *As*. Powder X-ray diffraction (PXRD) of the Cu_{17}NCs before and after interaction with As^{3+} reveals significant shifts in the diffraction

https://doi.org/10.1021/acs.estlett.4c00264
Environ. Sci. Technol. Lett. XXXX, XXX, XXX−XXX

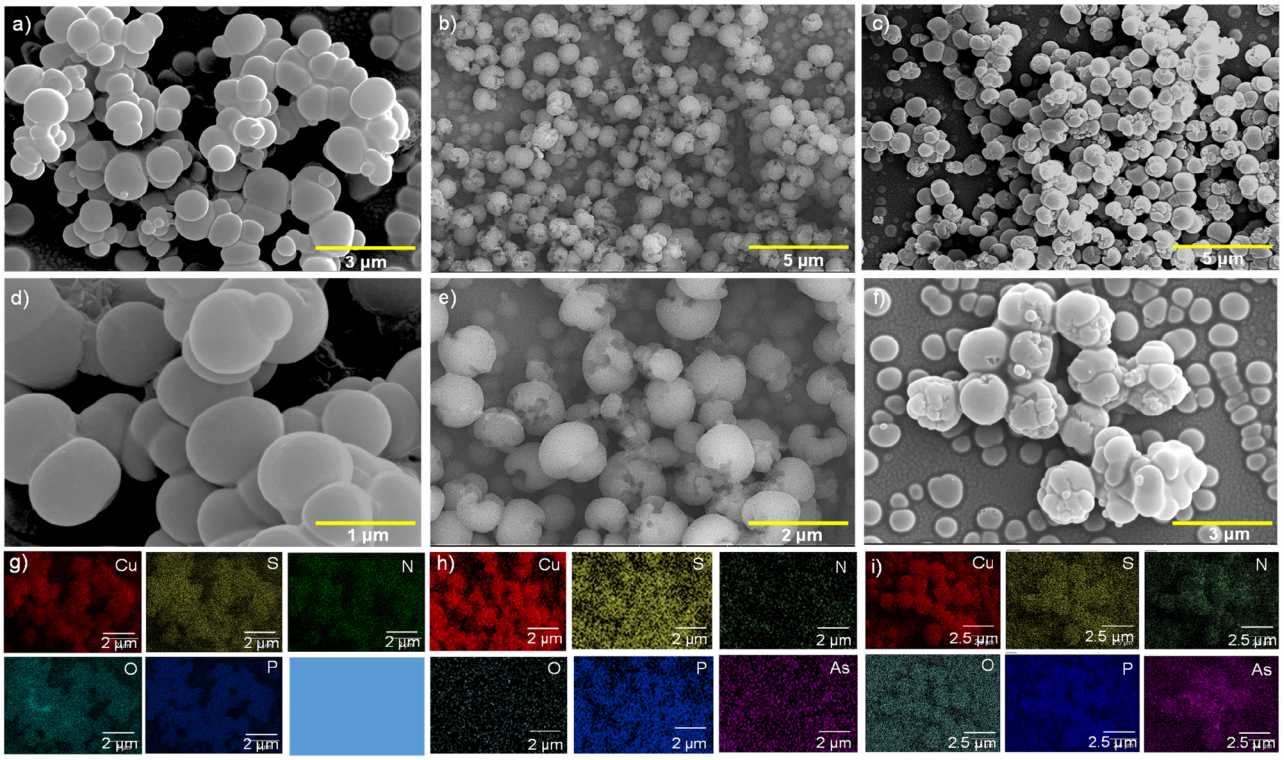

Figure 3. Morphological evolution induced by the *As* exposure to the CASs spheroids. FESEM micrographs showed (a) as prepared CASs and their disruption induced by the presence of (b) As^{3+} and (c) As^{5+}. Enlarged FESEM images show (d) smooth CASs and disrupted spheres after the exposure of (e) As^{3+} and (f) As^{5+}. EDS elemental maps of (g) untreated CASs spheres and after the exposure to (h) As^{3+} and (i) As^{5+}.

peaks and a notable decrease in intensity, particularly at 2θ values of 8.3°, 9.76° and 28° (Figure S8). While these peaks cannot be assigned in greater detail in the absence of the crystal structure, the observed peak shift and intensity reduction suggest a discernible alteration in the microcrystalline nature of Cu_{17}NCs.[30]

Impact of *As* on the Morphology of CASs. The formation of CuNC aggregates induced by solvophobic effect was monitored through dynamic light scattering (DLS) studies. The maximum aggregate size reached was ∼500 nm after 90 min of methanol addition to CuNCs solution in DCM (Figures S9a and b). Several reports exist on the prompt formation of aggregation-induced superstructures in CuNCs.[17,34,35] Time-dependent PL studies showed a maxima intensity at 643 nm due to the formation of aggregates after 120 min of LEIST reaction. (Figures S10a and b). Examining through field emission scanning electron microscope (FESEM), the CuNCs were observed to be self-assembled into a stable film composed of CASs, as shown in Figure 3a. Figure 3d provides a zoomed-in view of CASs. Nearly uniform spheroidal structures of approximately 500 nm were observed in the Cu_{17}NCs coating. These superstructures form due to the solvent interactions leading to aggregation, resulting in AIE in several systems. Similar solvent-induced aggregation has been reported by Jash et al. in forming superstructures of phosphine-protected Au−Ag alloy NCs.[36]

Upon exposure to 100 ppb of *As*, morphological changes were induced in the CASs, disrupting their shape. This alteration occurred after exposure to both As^{3+} (Figure 3b and zoomed-in view in Figure 3e) and As^{5+} (Figure 3c and zoomed-in view in Figure 3f). Energy-dispersive spectroscopy (EDS) maps of the CASs before (Figure 3g) and after adding As^{3+} (Figure 3h) and As^{5+} (Figure 3i) were recorded to confirm the composition of CASs and their interaction with *As*. The EDS maps illustrate the spatial distribution of Cu, S, O, N, P, and *As* elements. Cu of the cluster core was observed along with S, O, N and P present on the L-Cys and DPPE ligands. The spread of *As* on the disrupted CASs after exposure is evident from the EDS maps in Figures 3h and 3i.

Selectivity toward *As*. The CASs were found to be selective toward *As*, while they were unaffected by interfering heavy metal ions commonly present in contaminated water samples. The CASs were individually exposed to 100 ppb of Mn^{2+}, Cu^{2+}, Hg^{2+}, Pb^{2+}, Fe^{2+}, Cr^{2+}, Cd^{2+}, As^{3+} and As^{5+} in Milli-Q water. Photoluminescence (PL) was recorded after the exposure to individual ions of 100 ppb concentration (Figure S11a). The CASs exhibited emission quenching in the presence of As^{3+} and As^{5+}, as observed in Figure S11b. On the other hand, emission intensities remained constant when exposed to the interfering ions. The integrity of the microstructures in the presence of the interfering ions, such as Cr^{3+}, Fe^{2+} and Hg^{2+}, was examined through FESEM studies. The results, depicted in Figures S11c-f, revealed that the spheroidal morphology remained unaffected. A similar study on interfering ions involved tap water spiked with 100 ppb of Zn^{2+}, Pb^{2+}, Hg^{2+}, Cu^{2+}, Cd^{2+}, As^{3+} and As^{5+}. The recorded PL spectra showed that the emission intensity remained unaltered in the presence of the interfering ions, while quenching occurred solely in the presence of *As*, as shown in Figure S12. Additionally, Figure S12 displays photographs of the CASs-coated PP discs under UV light, captured after exposure to tap water containing ions of interest. This sensor interacts strongly with phosphate ions, but does not respond toward organic triphenyl arsine (TPA). (Figure S13). Phosphate removal

https://doi.org/10.1021/acs.estlett.4c00264
Environ. Sci. Technol. Lett. XXXX, XXX, XXX−XXX

agents will facilitate the practical application of the sensor in field samples.

Antibacterial and Antibiofilm Activity. The impact of CASs on both Gram-positive *Bacillus subtilis* and Gram-negative *Escherichia coli* was investigated. After interaction with the CASs coating, the number of viable bacterial cells was determined through colony counting (Figures S14a-d). The CASs-coated PP discs showed high bactericidal efficiency against *E. coli* and *B. subtilis* cells. The antibacterial activities observed against *E. coli* MTCC 443, *E. coli* MTCC 739, and *B. subtilis* were 97.8%, 98% and 95%, respectively (Figures S14e-g). At the same time, bare PP discs and PP discs coated with CuI, L-Cys, and solvent (methanol and DCM in 1:1 ratio) had significantly less or no effect on the bacteria. Environmental scanning electron microscope (ESEM) analysis was performed to understand the impact of CASs on bacterial cells. *E. coli* MTCC 443 cells exposed to CASs coating for 1 h (Figure S14h and zoomed in view in Figure S14i) showed cell membrane damage in comparison to control cells (Figure S14j and zoomed in view in Figure S14k) The cells exposed to CASs formed ghost cells as their contents appear to be released. Cell membrane damage was observed on the Gram-positive bacteria − *Staphylococcus aureus* and *B. subtilis* also (Figures S15 and S16, respectively). Several mechanisms have been reported for the antibacterial properties of NCs.[37] The thiolated ligand metal interface of the NCs induces higher antibacterial activity than free thiols, as they are prone to oxidation and tend to lose their stability.[27]

Coatings with cationic charges possess antibacterial effect on bacteria by electrostatic binding to the cell envelope, damaging the cells.[38] As discussed previously (Text S6), electrospray ionization mass spectrometry (ESI MS) analysis of the Cu_{17}NCs revealed their cationic nature, which could contribute to the net positive charge on the CASs surface. This was further analyzed through electrochemical impedance spectroscopy (EIS). We applied Mott−Schottky (M-S) analysis at the interface of the CASs-coated glassy carbon electrode (GCE) and the electrolyte (Figure S17a). The inverse square capacitance ($1/C_{sc}^2$) plot of CASs-coated film decreases with increasing potential.[39,40] From Figure S17b, it is evident that there is a sharp decrease of $1/C_{sc}^2$ value with an increase of the potential from −1 to +0.8 V, and the negative slope of the plot indicates that the coating is positively charged. However, the bare GCE shows a positive slope, indicating its negative charge. The extent of cell damage on the Gram-positive bacteria is lesser than that of *E. coli*. which carry a higher negative charge on the membrane of *E. coli*.[41,42]

Further, the antibiofilm-forming ability of the CASs was investigated using Gram-positive *B. subtilis* through ESEM. The bacteria formed biofilms on blank PP discs after 4 days (Figure S16a). On the other hand, biofilm was absent on CASs-coated PP discs (Figure S16b). The cell membrane damage inhibits anchoring of the cells to surfaces, preventing growth and the formation of biofilm-supporting extracellular matrices.

Such antibacterial and antibiofilm activity of CASs can also be attributed to their unique morphology. Nanostructures in the range of 500 nm prevent the growth of bacteria through size-induced effects.[43−45] This explains the adverse impact on *E. coli* cells and *B. subtilis* compared to *S. aureus*, whose cells are smaller and show comparatively lesser cell membrane damage under ESEM. Heckmann et al., in their experiments on nanostructures[45] showed that nanopillar arrays of polydimethylsiloxane possess bactericidal activity on *E. coli*, while *S. aureus* was repelled but not killed. Thus, it is evident that besides the surface charge and chemical composition, the morphology of the CASs plays a significant role in the antibacterial activity.

IMPLICATIONS

We present a novel application of CASs composed of Cu_{17}NCs exhibiting distinctive red luminescence as highly selective sensors for *As* in water. The sensitivity is extremely promising as it reaches one ppb. The CASs displayed remarkable specificity and selectivity toward *As* in water, showcasing their potential as efficient and affordable sensors for ensuring water safety on a global scale. In an era marked by increasing concerns about antibacterial resistance, our study also introduces a promising avenue for applying CASs systems as antibacterial surface coatings. These coatings exhibit a broad spectrum of killing efficiency attributed to the positive surface charge on the clusters, thiol functionalization, and nano-spherical structures. This unique combination contributes to their antibacterial efficacy and positions them as excellent antibiofilm platforms. While our findings represent a pioneering observation, suggesting the potential of Cu_{17} superstructures for detecting ultratrace levels of *As* and their application in antibacterial and antibiofilm-forming coatings, there is a need for additional studies on the temporal stability and applications in diverse conditions. We estimate that one water quality analysis using such a paper sensor would cost ∼ US $ 0.01 per test. Future research endeavors are essential to unravel the full spectrum of possibilities and refine the applications of CASs in addressing critical issues related to water safety and antibacterial resistance.

ASSOCIATED CONTENT

Supporting Information

The Supporting Information is available free of charge at https://pubs.acs.org/doi/10.1021/acs.estlett.4c00264.

More details regarding the methodology, characterization of nanoclusters (mass spectrometry and thermal stability analysis), photoluminescence measurements, electron microscopy, and relevant references (PDF)

AUTHOR INFORMATION

Corresponding Author

Thalappil Pradeep − *Department of Chemistry, DST Unit of Nanoscience (DST UNS) and Thematic Unit of Excellence (TUE), Indian Institute of Technology Madras, Chennai 600036, India;* orcid.org/0000-0003-3174-534X; Email: pradeep@iitm.ac.in

Authors

Jenifer Shantha Kumar − *Department of Chemistry, DST Unit of Nanoscience (DST UNS) and Thematic Unit of Excellence (TUE) and Department of Metallurgical and Materials Engineering, Indian Institute of Technology Madras, Chennai 600036, India;* orcid.org/0009-0003-7502-7005

Arijit Jana − *Department of Chemistry, DST Unit of Nanoscience (DST UNS) and Thematic Unit of Excellence (TUE), Indian Institute of Technology Madras, Chennai 600036, India*

https://doi.org/10.1021/acs.estlett.4c00264
Environ. Sci. Technol. Lett. XXXX, XXX, XXX−XXX

Jayathraa Raman − *Department of Chemistry, DST Unit of Nanoscience (DST UNS) and Thematic Unit of Excellence (TUE), Indian Institute of Technology Madras, Chennai 600036, India*

Hema Madhuri Veera − *Department of Chemistry, DST Unit of Nanoscience (DST UNS) and Thematic Unit of Excellence (TUE), Indian Institute of Technology Madras, Chennai 600036, India*

Amoghavarsha Ramachandra Kini − *Department of Chemistry, DST Unit of Nanoscience (DST UNS) and Thematic Unit of Excellence (TUE), Indian Institute of Technology Madras, Chennai 600036, India*

Jayoti Roy − *Department of Chemistry, DST Unit of Nanoscience (DST UNS) and Thematic Unit of Excellence (TUE), Indian Institute of Technology Madras, Chennai 600036, India*

Saurav Kanti Jana − *Department of Chemistry, DST Unit of Nanoscience (DST UNS) and Thematic Unit of Excellence (TUE), Indian Institute of Technology Madras, Chennai 600036, India;* orcid.org/0000-0001-5772-7022

Tiju Thomas − *Department of Metallurgical and Materials Engineering, Indian Institute of Technology Madras, Chennai 600036, India*

Complete contact information is available at: https://pubs.acs.org/10.1021/acs.estlett.4c00264

Notes

The authors declare no competing financial interest.

■ ACKNOWLEDGMENTS

The authors would like to acknowledge the Department of Science and Technology (DST), Government of India, for constantly supporting our research program. We have also utilized the funding from the project on the Centre of Excellence on Molecular Materials and Functions as part of the Institutes of Eminence scheme of IIT Madras. We thank the Science and Engineering Research Board (SERB) for the SUPRA (Scientific and Useful Profound Research Advancement) project Atomically Precise Materials for Sustainable Water and Energy Harvesting (SPR/2021/000439). J.S.K. thanks the Ministry of Human Resource Development, Government of India, for the senior research fellowship. J. Raman and H. M. Veera, from the Department of Biotechnology, Vel Tech High Tech Dr Rangarajan Dr Sakunthala Engineering College, Chennai 600062, India, had their internships with TP during the course of this work.

■ REFERENCES

(1) World Health Organization. https://www.who.int/news/item/18-06-2019-1-in-3-people-globally-do-not-have-access-to-safe-drinking-water-unicef-who (accessed Apr 3, 2024).

(2) Litter, M. I. Chemistry and Occurrence of Arsenic in Water. *Arsenic in Plants* **2022**, 25−48.

(3) German, M. S.; Watkins, T. A.; Chowdhury, M.; Chatterjee, P.; Rahman, M.; Seingheng, H.; SenGupta, A. K. Evidence of Economically Sustainable Village-Scale Microenterprises for Arsenic Remediation in Developing Countries. *Environ. Sci. Technol.* **2019**, *53* (3), 1078−1086.

(4) Mukherjee, S.; Gupte, T.; Jenifer, S. K.; Thomas, T.; Pradeep, T. Arsenic in Water: Fundamentals of Measurement and Remediation. *Encyclopedia of Water*. **2019**, 1−11.

(5) Kumar, A. A.; Som, A.; Longo, P.; Sudhakar, C.; Bhuin, R. G.; Gupta, S. S.; Anshup; Sankar, M. U.; Chaudhary, A.; Kumar, R.; Pradeep, T. Confined Metastable 2-Line Ferrihydrite for Affordable Point-of-Use Arsenic-Free Drinking Water. *Adv. Mater.* **2017**, *29* (7), No. 1604260.

(6) Babar, N. U. A.; Joya, K. S.; Tayyab, M. A.; Ashiq, M. N.; Sohail, M. Highly Sensitive and Selective Detection of Arsenic Using Electrogenerated Nanotextured Gold Assemblage. *ACS Omega* **2019**, *4* (9), 13645−13657.

(7) Bhanjana, G.; Dilbaghi, N.; Chaudhary, S.; Kim, K.-H.; Kumar, S. Robust and Direct Electrochemical Sensing of Arsenic Using Zirconia Nanocubes. *Analyst* **2016**, *141* (13), 4211−4218.

(8) Mukherjee, S.; Gupte, T.; Jenifer, S. K.; Thomas, T.; Pradeep, T. Arsenic in Water: Speciation, Sources, Distribution, and Toxicology. *Encyclopedia of Water* **2019**, 1−17.

(9) Goswami, N.; Giri, A.; Bootharaju, M. S.; Xavier, P. L.; Pradeep, T.; Pal, S. K. Copper Quantum Clusters in Protein Matrix: Potential Sensor of Pb2+ Ion. *Anal. Chem.* **2011**, *83* (24), 9676−9680.

(10) Nagar, A.; Pradeep, T. Clean Water through Nanotechnology: Needs, Gaps, and Fulfillment. *ACS Nano* **2020**, *14* (6), 6420−6435.

(11) Pradeep, T. Atomically Precise Clusters of Noble Metals: An Introduction. In *Atomically Precise Metal Nanoclusters*; Pradeep, T., Ed.; Elsevier, 2023; pp 1−5. DOI: 10.1016/B978-0-323-90879-5.00008-1.

(12) Jana, A.; Kini, A. R.; Pradeep, T. Atomically Precise Clusters: Chemical Evolution of Molecular Matter at the Nanoscale. *AsiaChem. Mag.* **2023**, *3* (1), 56−65.

(13) Chakraborty, I.; Pradeep, T. Atomically Precise Clusters of Noble Metals: Emerging Link between Atoms and Nanoparticles. *Chem. Rev.* **2017**, *117* (12), 8208−8271.

(14) Lin, Y.-S.; Lin, Y.-F.; Nain, A.; Huang, Y.-F.; Chang, H.-T. A Critical Review of Copper Nanoclusters for Monitoring of Water Quality. *Sensors and Actuators Reports* **2021**, *3*, No. 100026.

(15) Baghdasaryan, A.; Bürgi, T. Copper Nanoclusters: Designed Synthesis, Structural Diversity, and Multiplatform Applications. *Nanoscale* **2021**, *13* (13), 6283−6340.

(16) Zhou, C.; Wang, M.; Yao, Q.; Zhou, Y.; Hou, C.; Xia, J.; Wang, Z.; Chen, J.; Xie, J. Ligand-Dependent Aggregation-Enhanced Photoacoustic of Atomically Precise Metal Nanocluster. *Aggregate* **2023**, *5* (1), No. e401.

(17) Chen, P.-C.; Li, Y.-C.; Ma, J.-Y.; Huang, J.-Y.; Chen, C.-F.; Chang, H.-T. Size-Tunable Copper Nanocluster Aggregates and Their Application in Hydrogen Sulfide Sensing on Paper-Based Devices. *Sci. Rep.* **2016**, *6* (1), 24882.

(18) Xiao, X.-Y.; Song, Z.-Y.; Li, P.-H.; Chen, S.-H.; Li, L.-N.; Yang, M.; Lin, C.-H.; Huang, X.-J. Au25 Nanoclusters Exhibit Superhigh Catalytic Activity in Electrochemical Detection of As(III). *Anal. Chem.* **2021**, *93* (41), 14014−14023.

(19) Jose, A.; Jana, A.; Gupte, T.; Nair, A. S.; Unni, K.; Nagar, A.; Kini, A. R.; Spoorthi, B. K.; Jana, S. K.; Pathak, B.; Pradeep, T. Vertically Aligned Nanoplates of Atomically Precise Co6S8 Cluster for Practical Arsenic Sensing. *ACS Mater. Lett.* **2023**, *5* (3), 893−899.

(20) Nain, A.; Tseng, Y.-T.; Lin, Y.-S.; Wei, S.-C.; Mandal, R. P.; Unnikrishnan, B.; Huang, C.-C.; Tseng, F.-G.; Chang, H.-T. Tuning the Photoluminescence of Metal Nanoclusters for Selective Detection of Multiple Heavy Metal Ions. *Sensors Actuators B Chem.* **2020**, *321*, No. 128539.

(21) Roy, S.; Palui, G.; Banerjee, A. The As-Prepared Gold Cluster-Based Fluorescent Sensor for the Selective Detection of AsIII Ions in Aqueous Solution. *Nanoscale* **2012**, *4* (8), 2734−2740.

(22) Qian, S.; Wang, Z.; Zuo, Z.; Wang, X.; Wang, Q.; Yuan, X. Engineering Luminescent Metal Nanoclusters for Sensing Applications. *Coord. Chem. Rev.* **2022**, *451*, No. 214268.

(23) Yuan, L.; Liang, M.; Hummel, M.; Shao, C.; Lu, S. Rational Design Copper Nanocluster-Based Fluorescent Sensors towards Heavy Metal Ions: A Review. *Chemosensors.* **2023**, *11*, 159−162.

(24) Antibiotic resistance threats in the united states 2019. https://www.cdc.gov/drugresistance/pdf/threats-report/2019-ar-threats-report-508.pdf (accessed Apr 3, 2024).

(25) Kannan, U.; Pullangott, G.; Singh, S. P.; Maliyekkal, S. M. *5 - Nanoscale Silver Enabled Drinking Water Disinfection System*; Hussain,

C. M., Nassar, N. N., Eds.; Elsevier, 2023; pp 127−166. DOI: 10.1016/B978-0-12-823874-5.00010-3.
(26) Chakraborty, I.; Udayabhaskararao, T.; Deepesh, G. K.; Pradeep, T. Sunlight Mediated Synthesis and Antibacterial Properties of Monolayer Protected Silver Clusters. *J. Mater. Chem. B* **2013**, *1* (33), 4059−4064.
(27) Nain, A.; Tseng, Y.-T.; Wei, S.-C.; Periasamy, A. P.; Huang, C.-C.; Tseng, F.-G.; Chang, H.-T. Capping 1,3-Propanedithiol to Boost the Antibacterial Activity of Protein-Templated Copper Nanoclusters. *J. Hazard. Mater.* **2020**, *389*, No. 121821.
(28) Raffi, M.; Mehrwan, S.; Bhatti, T. M.; Akhter, J. I.; Hameed, A.; Yawar, W.; ul Hasan, M. M. Investigations into the Antibacterial Behavior of Copper Nanoparticles against Escherichia Coli. *Ann. Microbiol.* **2010**, *60* (1), 75−80.
(29) Li, J.; Ma, H. Z.; Reid, G. E.; Edwards, A. J.; Hong, Y.; White, J. M.; Mulder, R. J.; O'Hair, R. A. J. Synthesis and X-Ray Crystallographic Characterisation of Frustum-Shaped Ligated [Cu18H16(DPPE)6]2+ and [Cu16H14(DPPA)6]2+ Nanoclusters and Studies on Their H2 Evolution Reactions. *Chem. − A Eur. J.* **2018**, *24* (9), 2070−2074.
(30) Jana, A.; Spoorthi, B. K.; Nair, A. S.; Nagar, A.; Pathak, B.; Base, T.; Pradeep, T. A Luminescent Cu4 Cluster Film Grown by Electrospray Deposition: A Nitroaromatic Vapour Sensor. *Nanoscale* **2023**, *15* (18), 8141−8147.
(31) Kumar, S.; Bhanjana, G.; Dilbaghi, N.; Kumar, R.; Umar, A. Fabrication and Characterization of Highly Sensitive and Selective Arsenic Sensor Based on Ultra-Thin Graphene Oxide Nanosheets. *Sensors Actuators B Chem.* **2016**, *227*, 29−34.
(32) Yang, M.; Jiang, T.-J.; Wang, Y.; Liu, J.-H.; Li, L.-N.; Chen, X.; Huang, X.-J. Enhanced Electrochemical Sensing Arsenic(III) with Excellent Anti-Interference Using Amino-Functionalized Graphene Oxide Decorated Gold Microelectrode: XPS and XANES Evidence. *Sensors Actuators B Chem.* **2017**, *245*, 230−237.
(33) Vaishanav, S. K.; Korram, J.; Pradhan, P.; Chandraker, K.; Nagwanshi, R.; Ghosh, K. K.; Satnami, M. L. Green Luminescent CdTe Quantum Dot Based Fluorescence Nano-Sensor for Sensitive Detection of Arsenic (III). *J. Fluoresc.* **2017**, *27* (3), 781−789.
(34) Zheng, X.; Chen, Q.; Zhang, Z.; Wang, Z.; Gong, Z. An Aggregation-Induced Emission Copper Nanoclusters Fluorescence Probe for the Sensitive Detection of Tetracycline. *Microchem. J.* **2022**, *180*, No. 107570.
(35) Jia, X.; Li, J.; Wang, E. Cu Nanoclusters with Aggregation Induced Emission Enhancement. *Small* **2013**, *9* (22), 3873−3879.
(36) Jash, M.; Jana, A.; Poonia, A. K.; Khatun, E.; Chakraborty, P.; Nagar, A.; Ahuja, T.; Adarsh, K. V.; Pradeep, T. Phosphine-Protected Atomically Precise Silver−Gold Alloy Nanoclusters and Their Luminescent Superstructures. *Chem. Mater.* **2023**, *35* (1), 313−326.
(37) Li, D.; Kumari, B.; Makabenta, J. M.; Tao, B.; Qian, K.; Mei, X.; Rotello, V. M. Development of Coinage Metal Nanoclusters as Antimicrobials to Combat Bacterial Infections. *J. Mater. Chem. B* **2020**, *8* (41), 9466−9480.
(38) Li, Y.; Qu, S.; Xue, Y.; Zhang, L.; Shang, L. Cationic Antibacterial Metal Nanoclusters with Traceable Capability for Fluorescent Imaging the Nano—Bio Interactions. *Nano Res.* **2023**, *16* (1), 999−1008.
(39) Jana, S. K.; Banerjee, S.; Bayan, S.; Inta, H. R.; Mahalingam, V. Rectification and Amplification of Ionic Current in Planar Graphene/Graphene-Oxide Junctions: An Electrochemical Diode and Transistor. *J. Phys. Chem. C* **2018**, *122* (21), 11378−11384.
(40) Jana, S. K.; Chaudhari, K.; Islam, M. R.; Natarajan, G.; Ahuja, T.; Som, A.; Paramasivam, G.; Raghavendra, A.; Sudhakar, C.; Pradeep, T. Selective and Practical Graphene-Based Arsenite Sensor at 10 Ppb. *ACS Appl. Nano Mater.* **2022**, *5* (8), 11876−11888.
(41) Chai, S.; Zhou, L.; Chi, Y.; Chen, L.; Pei, S.; Chen, B. Enhanced Antibacterial Activity with Increasing P Doping Ratio in CQDs. *RSC Adv.* **2022**, *12* (43), 27709−27715.
(42) Ahimou, F.; Denis, F. A.; Touhami, A.; Dufrêne, Y. F. Probing Microbial Cell Surface Charges by Atomic Force Microscopy. *Langmuir* **2002**, *18* (25), 9937−9941.
(43) Fadeeva, E.; Truong, V. K.; Stiesch, M.; Chichkov, B. N.; Crawford, R. J.; Wang, J.; Ivanova, E. P. Bacterial Retention on Superhydrophobic Titanium Surfaces Fabricated by Femtosecond Laser Ablation. *Langmuir* **2011**, *27* (6), 3012−3019.
(44) Francesko, A.; Fernandes, M. M.; Ivanova, K.; Amorim, S.; Reis, R. L.; Pashkuleva, I.; Mendoza, E.; Pfeifer, A.; Heinze, T.; Tzanov, T. Bacteria-Responsive Multilayer Coatings Comprising Polycationic Nanospheres for Bacteria Biofilm Prevention on Urinary Catheters. *Acta Biomater.* **2016**, *33*, 203−212.
(45) Heckmann, T. S.; Schiffman, J. D. Spatially Organized Nanopillar Arrays Dissimilarly Affect the Antifouling and Antibacterial Activities of Escherichia Coli and Staphylococcus Aureus. *ACS Appl. Nano Mater.* **2020**, *3* (2), 977−984.

https://doi.org/10.1021/acs.estlett.4c00264
Environ. Sci. Technol. Lett. XXXX, XXX, XXX−XXX